Heliyon 10 (2024) e24204

Contents lists available at ScienceDirect

Heliyon

journal homepage: www.cell.com/heliyon

Research article

Downregulating ANGPTL3 by miR-144-3p promoted TGF-β1-induced renal interstitial fibrosis via activating PI3K/AKT signaling pathway

Bin Yang [a,1], Fengxian Shen [b,1], Yi Zhu [a], Haolei Cai [a,*]

[a] Department of Hepato-Pancreato-Biliary Surgery, The Second Affiliated Hospital, Zhejiang University School of Medicine, Hangzhou, Zhejiang, 310009, China

[b] Department of Reproductive Endocrinology, Women's Hospital, Zhejiang University School of Medicine, Hangzhou, Zhejiang, 310006, China

ARTICLE INFO

Keywords:
Renal interstitial fibrosis
ANGPTL3
miR-144-3p
PI3K
AKT

ABSTRACT

Despite observations of decreased ANGPTL3 (angiopoietin-like protein 3) levels in tubular atrophy and renal interstitial fibrosis (RIF), its functional implications and regulatory mechanisms in RIF remain unclear. This investigation employed unilateral ureteral obstruction (UUO) mice as *in vivo* model and human proximal kidney tubuloepithelial HK-2 cells under TGF-β1 treatment as *in vitro* model to explore RIF. The RIF extent was evaluated using H & E staining and Masson's trichrome staining. There was a significant decrease in ANGPTL3 levels and an increase in miR-144-3p, accompanied by heightened expressions of α-SMA, p-PI3K, p-AKT, Collagen I, and Fibronectin in the UUO mice and HK-2 cells treated with TGF-β1. Enhancing ANGPTL3 expression or suppressing miR-144-3p mitigated TGF-β1-induced cellular apoptosis, inflammation, and PI3K/AKT signaling pathway activation, as evidenced by altered levels of α-SMA, Collagen I, Fibronectin, and associated signaling markers. Using a bioinformatics approach, a miR-144-3p binding site was discovered on the ANGPTL3 mRNA, and this finding was subsequently confirmed through luciferase reporter assay. In HK-2 cells stimulated with TGF-β1, the suppression of ANGPTL3 negated the effects of inhibiting miR-144-3p. Under comparable conditions, the use of LY294002, an inhibitor of the PI3K/AKT pathway, nullified the effects caused by the knockdown of ANGPTL3. Collectively, these findings indicate that miR-144-3p exacerbates RIF through PI3K/AKT pathway activation by targeting ANGPTL3, highlighting a novel potential therapeutic target for RIF management.

1. Introduction

Renal interstitial fibrosis (RIF), a pivotal stage in the progression from CKD (chronic kidney disease) to ESRD (end-stage renal disease), is marked by an excessive accumulation of extracellular matrix proteins, the infiltration of inflammatory cells, and increased apoptosis in tubular epithelial cells [1]. Current therapeutic approaches for RIF are multifaceted, involving renin-angiotensin system inhibitors and lipid-lowering agents for blood pressure control, coupled with stringent dietary modifications [2,3]. While these

* Corresponding author. Department of Hepato-Pancreato-Biliary Surgery, the Second Affiliated Hospital, Zhejiang University School of Medicine, No.88 Jiefang Road, Shangcheng District, Hangzhou, Zhejiang, 310009, China.
E-mail address: cai_haolei203@126.com (H. Cai).
[1] Contributed to this work equally.

https://doi.org/10.1016/j.heliyon.2024.e24204
Received 25 July 2023; Received in revised form 4 January 2024; Accepted 4 January 2024
Available online 8 January 2024

measures have shown efficacy in preserving renal function, the incidence of ESRD continues to be substantial [4]. Consequently, it is imperative to delve deeper into the molecular underpinnings of renal fibrosis to formulate more effective treatment modalities.

ANGPTL3 (Angiopoietin-like protein 3), predominantly produced by the liver, is a versatile protein with distinct functional domains. Its coiled-coil domain (CCD) plays a pivotal role in lipid metabolism regulation, while the fibrinogen-like domain (FLD) is instrumental in angiogenesis, primarily through interaction with the integrin αvβ3 receptor [5]. ANGPTL3's involvement in various renal pathologies, including diabetic nephropathy [6], renal cell carcinoma [7] and acute kidney injury [8] has been documented. From a bioinformatics perspective, Yang et al. [9] identified ANGPTL3 as a crucial diagnostic gene connected to immune and renal disease-related pathways. This aligns with findings by Maluf et al. [10], who in their genomic study observed a downregulation of angiogenesis-associated genes, including ANGPTL3, ANGPT2, and VEGF, in conditions of tubular atrophy and interstitial fibrosis. Additionally, research has noted elevated levels of ANGPTL3 in the renal tissues of children with minimal change nephrotic syndrome, which affects the functional integrity of human glomerular endothelial cells through the PI3K/AKT pathway [11]. In hemodialysis patients, there's a reported increase in plasma levels of ANGPTL3 and ANGPTL4, undergoing changes following tinzaparin administration [12]. Moreover, the observed decrease in ANGPTL3 levels in hemodialysis patients, and its association with key elements of uremic dyslipidemia, suggests a potential role in the pathology of this condition [13]. Although research into ANGPTL3 is extensive, its precise influence on the development of RIF remains to be fully elucidated.

A multitude of research has emphasized the vital roles of miRNAs in various biological processes, especially in the advancement of renal fibrosis [14,15]. Our previous investigations have identified ANGPTL3 as a likely target of miR-144-3p, a finding supported by predictions from the TargetScan database. Studies on idiopathic pulmonary fibrosis (IPF) have shown an increase in miR-144-3p levels in IPF fibroblasts, with its subsequent decrease linked to reduced α-SMA expression in these cells [16]. Additionally, Yuan et al. [17] discovered that miR-144-3p′s modulation of PTEN may represent a promising therapeutic approach for cardiac fibrosis post-myocardial infarction. Drawing on these insights, we hypothesize that targeting ANGPTL3 using miR-144-3p could emerge as an effective therapeutic strategy for CKD.

Consequently, this research was primarily focused on validating the complementary interaction between miR-144-3p and ANGPTL3 and investigating the functional implications of the miR-144-3p/ANGPTL3 axis in the progression of RIF.

2. Materials and methods

2.1. UUO model

Male C57BL/6 mice, aged 8 weeks and weighing between 20 and 25 g, were sourced from the Shanghai Laboratory Animal Center, part of the Chinese Academy of Sciences (Shanghai, China). The mice were housed under controlled conditions, including a consistent temperature of 21 °C ± 2 °C, 12-h alternating light and dark cycles, and maintained humidity levels of 55 % ± 2 %. The RIF mouse model (n = 5) was created by conducting UUO surgery, adhering to methods detailed in prior studies [18,19]. In brief, the mice were administered an anesthetic dose of pentobarbital (75 mg/kg, intraperitoneally), followed by a unilateral abdominal incision to expose the left ureter, which was then securely double ligated using 4-0 silk sutures. The sham group of mice (n = 5) was subjected to a procedure mirroring that of the UUO group, excluding the ureter ligation step. Fourteen days post-surgery, the left kidney, exhibiting hydronephrosis, was harvested from these mice for subsequent pathological and molecular evaluations. The protocols for all animal experiments received approval from the Animal Ethics Committee at Zhejiang University School of Medicine, ensuring compliance with the Zhejiang University School of Medicine's guidelines for the Use and Care of Experimental Animals (Approval No. ZUS-87DT).

2.2. Histological staining

Kidney specimens were preserved in 10 % buffered formalin, set in paraffin, and transversely sliced into 4 μm thick sections. These sections were then deparaffinized using xylene and rehydrated through a series of ethanol solutions. Kidney tubular injuries were highlighted using a hematoxylin–eosin (H&E) staining kit (Solarbio, Beijing, China). This involved staining with hematoxylin for 5 min, followed by a bluing process in 0.2 % ammonia water or saturated lithium carbonate solution for 30 s. The sections were subsequently rinsed with 70 % and 90 % alcohol and counterstained with eosin-phloxine for 2 min. Renal interstitial lesions were evaluated using a modified Masson's trichrome stain kit (Solarbio, Beijing, China), adhering to the manufacturer's guidelines. All stained images were captured using a Nikon ECLIPSE 80i microscope in Japan.

2.3. Cell treatment

The HK-2 human proximal kidney tubuloepithelial cell line (Cat No. CRL-2190) was sourced from the ATCC (Manassas, VA, USA). These HK-2 cells were grown in DMEM/F12 medium enriched with 10 % fetal bovine serum, 1 % penicillin, and 1 % streptomycin (Gibco, USA), and kept in a humidified incubator at 37 °C with CO_2. For simulating TGF-β1-induced fibrosis, HK-2 cells were plated in a 24-well plate until they reached 50–60 % confluence and then switched to serum-free medium for 24 h. Subsequently, the cells were treated with 10 ng/mL TGF-β1 (PeproTech, Rocky Hill, USA) for 48 h. To examine the role of the PI3K/AKT signaling pathway in this context, the cells were also treated with 10 μM LY294002, a specific inhibitor of this pathway, for 24 h.

2.4. Cell transfection

HK-2 cells were plated in six-well plates at a density of 5×10^5 cells per well and allowed to grow until they were about 80 % confluent. Following this, the cells underwent transfection with various agents: 40 nM pcDNA3.1-ANGPTL3 plasmid, a miR-144-3p inhibitor, a negative control (miR-NC), small interfering RNA specific for ANGPTL3 (si-ANGPTL3), si-NC, or a combination of miR-144-3p inhibitor and si-ANGPTL3, all obtained from RiboBio (Guangzhou, China). This transfection process was carried out using Lipofectamine 2000 (Invitrogen, USA), in accordance with the guidelines provided by the manufacturer. Post-transfection, the cells were treated with 10 ng/mL TGF-β1 and LY294002.

2.5. Luciferase reporter assay

The potential interaction between the 3′-untranslated region (3′-UTR) of ANGPTL3 and miR-144-3p was predicted using the TargetScan platform (https://www.targetscan.org/vert_80/). This was experimentally verified through luciferase reporter assay. The assay used synthetic versions of both the wild-type (WT) and mutant-type (MUT) seed regions of ANGPTL3, inserted into the pMIR vector (by Promega Corporation, Madison, WI, USA). To assess the impact of miR-144-3p on ANGPTL3, HK-2 cells underwent co-transfection with either a miR-144-3p inhibitor or a miR-NC, in combination with either pMIR-ANGPTL3-WT or pMIR-ANGPTL3-MUT, employing Lipofectamine 2000 (Invitrogen, USA) at a temperature of 37 °C. After incubating for 48 h, the cell lysates were collected for analysis. The measurement of relative luciferase activity (firefly versus renilla luciferase fluorescence ratio) was conducted using the Dual-Luciferase Reporter Assay System from Promega Corporation, adhering to the manufacturer's guidelines.

2.6. ELISA assay

Post-treatment, supernatants from the HK-2 cell groups were collected, centrifuged at 3000 rpm for 15 min, and then stored at 4 °C for future analysis. To measure the levels of TNF-α and IL-6 in the HK-2 cell supernatant, commercially available ELISA kits for TNF-α (ab100654, Abcam, Cambridge, MA, USA) and IL-6 (ab178013, Abcam) were employed, with 10 μl of the sample added to each well of a 96-well plate. The optical density (OD) readings were obtained using an automated microplate reader at 450 nm. This was calibrated against a range of diluted antibodies in the medium, varying from 10 to 2000 pg/mL, to generate standard curves. Each sample was tested in triplicate, and the entire process was repeated three times.

2.7. Assessment of cell apoptosis

To determine the rate of apoptosis in HK-2 cells, the Annexin V/PI kit (KeyGEN Biotech, Nanjing, China, #KGA1026) was utilized. Initially, HK-2 cells from various groups were cultured in six-well plates at 1.0×10^5 cells per well, rinsed with PBS, and then resuspended in 100 μl of 1× binding buffer. Subsequently, the cells were treated with 5 μl of Annexin V-FITC for 15 min at ambient temperature in a dark environment. Following this, the cells were washed and resuspended in 200 μl of 1× binding buffer, and then 5 μl of PI solution was added for an additional 15 min. The apoptotic rate in each group of cells was then assessed using FACScan flow cytometry (BD Biosciences, San Jose, CA, USA), equipped with CellQuest software (Verity Software House, Maine, USA).

2.8. Quantitative real-time PCR

Total RNA was extracted using TRIzol reagent (#15596-026, Invitrogen, Carlsbad, CA, USA), followed by reverse transcription using a miRNA reverse transcription kit (Thermo Fisher Scientific, Inc.) adhering to the provided guidelines. Quantitative real-time PCR was then conducted using SYBR Premix Ex Taq (Takara, Tokyo, Japan) on an ABI Prism 7500 RT PCR system (Applied Biosystems, Foster City, CA, USA). The primers used were as follows: for mmu-miR-144-3p, forward: 5′-TACAGTATAGATGATGTACT-3′, reverse: 5′-GAACATGTCTGCGTATCTC-3′; for mmu-U6, forward: 5′-GCATGACGTCTGCTTTGGA-3′, reverse: 5′-CCA-CAATCATTCTGCCATCA-3′; for hsa-miR-144-3p, forward: 5′-GGATATCATCATATACTGTA-3′, reverse: 5′-GAACATGTCTGCGTATCTC-3′; for hsa-U6, forward: 5′-CTCGCTTCGGCAGCACA-3′, reverse: 5′-AACGCTTCAGGAATTTGCGT-3′; for mmu-ANGPTL3, forward: 5′-GGAAAGATGGCTCACAGGACT-3′, reverse: 5′- TCAACGTAGTGCTTGCTGTCT-3′; and for mmu-GAPDH, forward: 5′-TGGTGAAGGTCGGTGTGAAC-3′, reverse: 5′-TTCCCATTCTCGGCCTTGAC-3′. The PCR cycling conditions were set as follows: an initial denaturation at 95 °C for 30 s, followed by 40 cycles of 95 °C for 5 s and 60 °C for 30 s. The $2^{-\Delta\Delta Ct}$ method [20] was used to calculate the relative expression levels of miR-144-3p, normalized against U6.

2.9. Western blot analysis

Total protein from kidney tissues and cells across different groups was extracted using cold RIPA lysis buffer (Thermo Fisher Scientific, Inc.). The protein concentrations were then determined using a BCA protein assay kit (Beyotime). For the protein analysis, 30 μg of each protein sample was subjected to 8–12 % SDS-PAGE. Following the electrophoresis, proteins were transferred to PVDF membranes, which were subsequently blocked with 5 % non-fat dry milk for 2 h at 37 °C to minimize nonspecific binding. The membranes were then incubated overnight at 4 °C with primary antibodies: ANGPTL3 (1:1000; cat. no. ab118208, Abcam, Cambridge, UK), α-SMA (1:500; cat. no. ab5694), PI3K (1:1000; cat. no. ab302958), p-PI3K (1:500; cat. no. ab182651), AKT (1:500, cat. no. ab8805), p-AKT (1:500, cat. no. ab38449), Collagen I (1:1000, ab21286) and Fibronectin (1:1000, ab199056) and GAPDH (1:1000;

cat. no. ab9485). This was followed by a 1-h incubation at room temperature with a horseradish peroxidase-conjugated goat anti-rabbit secondary antibody (1:1000; cat. no. ab150077; Abcam). Protein bands were visualized using an ECL substrate kit (Millipore Corporation, Boston, MA, USA).

2.10. Statistical analysis

Quantitative data in this study are shown as means ± standard deviation (SD), based on a minimum of three independent experiments. Statistical analyses were performed using GraphPad Prism Version 8.0 (GraphPad Software, Inc., La Jolla, CA, USA). Differences between two groups were assessed using Student's t-test, while one-way ANOVA followed by Tukey's post-test was used for comparisons among multiple groups. A *p*-value of less than 0.05 was considered statistically significant.

3. Results

3.1. Expression levels of miR-144-3p, ANGPTL3 and PI3K/AKT pathway markers in UUO mouse model

In our experiment to create a renal fibrosis model, C57BL/6J mice underwent UUO. Kidney samples from these mice, as illustrated in Fig. 1A, exhibited significant pathological alterations, including enlarged renal and interstitial tubules, infiltration by inflammatory cells, and apoptosis of tubular cells, especially when contrasted with the sham-operated group. Masson's trichrome staining, as shown in Fig. 1B, revealed markedly increased blue collagen accumulation in the UUO group's kidneys relative to the sham group. Through quantitative real-time PCR analysis, we noted a notable elevation in miR-144-3p expression (Fig. 1C) and a reduction in ANGPTL3 expression (Fig. 1D) in the UUO group's kidney tissues compared to the sham group. Additionally, we observed lowered ANGPTL3 protein levels and heightened protein levels of fibrosis-related markers (α-SMA, Collagen I, and Fibronectin) as well as PI3K/AKT pathway markers (p-PI3K and p-AKT) in the fibrosis (UUO) group versus the sham group (Fig. 1E).

3.2. Elevating ANGPTL3 levels mitigated the inflammation, fibrosis, and PI3K/AKT pathway activation induced by TGF-β1 in HK-2 cells

To explore ANGPTL3's role in renal fibrosis *in vitro*, we transfected HK-2 cells with pcDNA3.1-ANGPTL3 or a pcDNA3.1 empty vector. As shown in Fig. 2A, HK-2 cells transfected with pcDNA3.1-ANGPTL3 exhibited a marked increase in ANGPTL3 protein

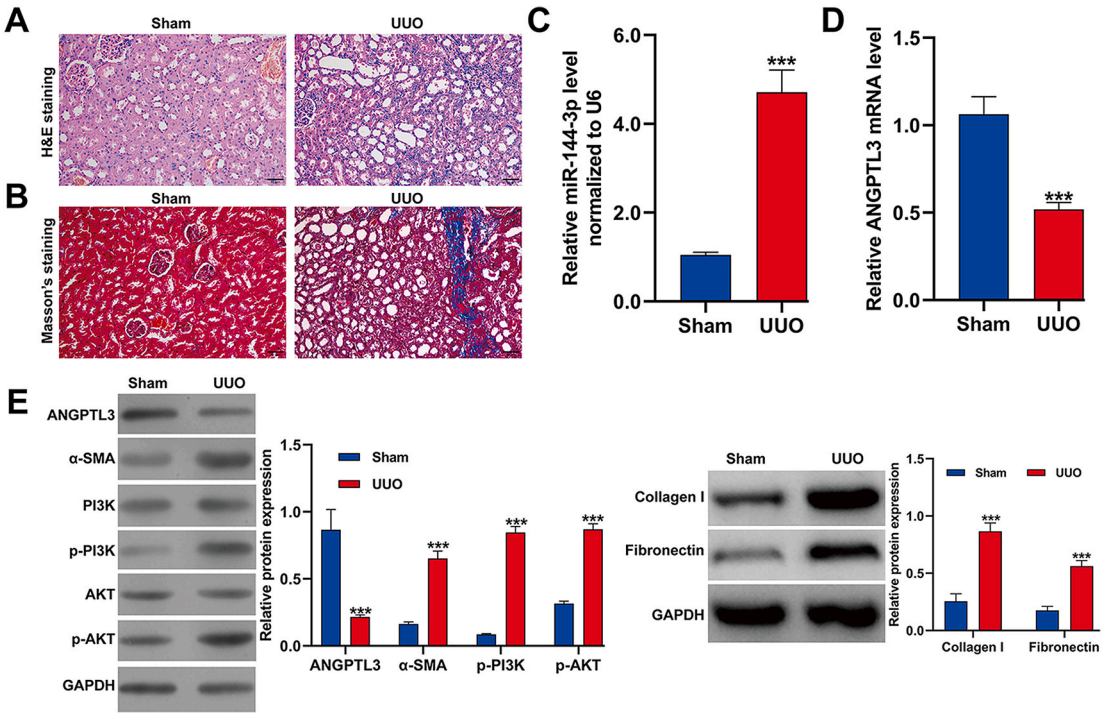

Fig. 1. Expression levels of miR-144-3p, ANGPTL3 and PI3K/AKT pathway markers in UUO mouse model. Representative micrographs of hematoxylin–eosin (H&E) staining (A) and Masson trichrome staining (B) in kidney tissues derived from UUO and sham group with five mice in each group. Scale bars, 100 μm; (C–D) Quantitative real-time PCR-based expressions of miR-144-3p and ANGPTL3 in the sham and UUO groups, and the internal reference miRNA was U6. Data were expressed as means ± SD. ***$p < 0.001$, compared with sham; (E) Western blot results including ANGPTL3, α-SMA, PI3K, p-PI3K, AKT, p-AKT, Collagen I and Fibronectin in the sham and UUO groups. GAPDH was used as an internal reference for the other proteins.

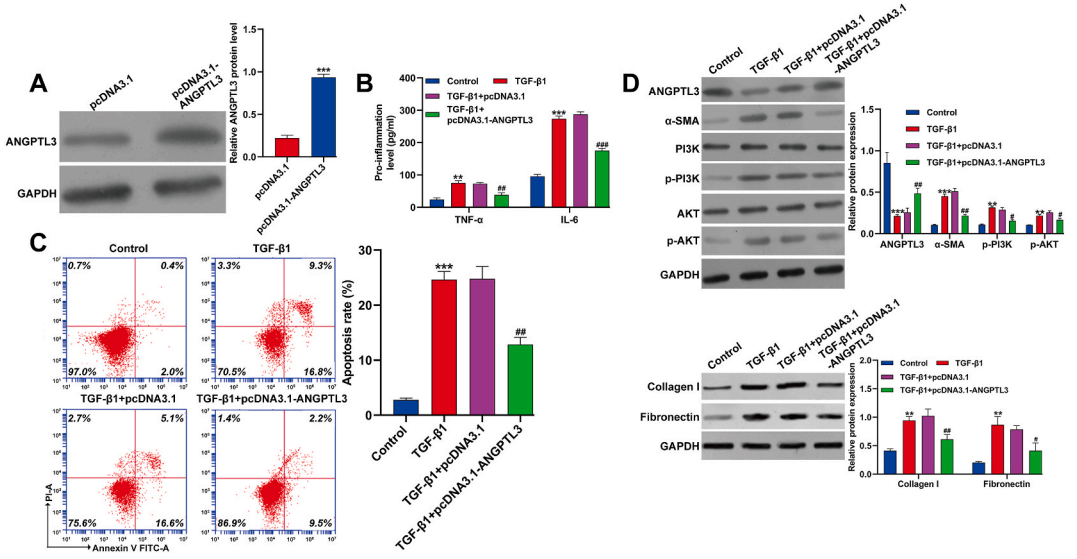

Fig. 2. Elevating ANGPTL3 levels mitigated the inflammation, fibrosis, and PI3K/AKT pathway activation induced by TGF-β1 in HK-2 cells. (A) The protein level of ANGPTL3 was determined in HK-2 cells after transfection with pcDNA3.1-ANGPTL3 or pcDNA3.1. HK-2 cells were transfected with pcDNA3.1-ANGPTL3 or pcDNA3.1, followed by treatment with 10 ng/mL TGF-β1. $***p < 0.001$, compared with pcDNA3.1; (B) ELISA assay was used to determine the concentration levels of TNF-α and IL-6 in the above HK-2 cells. (C) Cell apoptotic rate was measured in the above HK-2 cells. (D) The protein levels of ANGPTL3, α-SMA, PI3K, p-PI3K, AKT, p-AKT, Collagen I and Fibronectin were detected in the above HK-2 cells via Western blot analysis. Data were expressed as means ± SD. $**p < 0.01$, $***p < 0.001$, compared with control; $\#p < 0.05$, $\#\#p < 0.01$, $\#\#\#p < 0.001$, compared with TGF-β1 + pcDNA3.1.

expression compared to those with the pcDNA3.1 control. Overexpressing ANGPTL3 significantly reduced the TGF-β1-induced elevation of pro-inflammatory factors TNF-α and IL-6 in HK-2 cells, as depicted in Fig. 2B. Flow cytometry results, presented in Fig. 2C, indicated that ANGPTL3 overexpression notably decreased TGF-β1-induced apoptosis in HK-2 cells. Western blot analysis, as detailed in Fig. 2D, showed that ANGPTL3 overexpression counteracted the TGF-β1-induced decrease in ANGPTL3 and increase in α-SMA, Collagen I, and Fibronectin expression, along with the upregulation of PI3K/AKT pathway markers, p-PI3K and p-AKT. These results suggest that upregulating ANGPTL3 may inhibit TGF-β1-induced renal fibrosis through the initiation of the PI3K/AKT pathway.

3.3. ANGPTL3 identified as a direct target of miR-144-3p

To explore the post-transcriptional regulation mechanisms of ANGPTL3 gene expression in RIF, we used the TargetScan database to predict microRNAs that might regulate ANGPTL3. Fig. 3A shows that the ANGPTL3 gene has a potential miR-144-3p binding site in its 3′-UTR. A luciferase reporter assay was performed to confirm the direct interaction between miR-144-3p and the 3′-UTR of ANGPTL3. The assay revealed that the miR-144-3p inhibitor significantly enhanced luciferase activity in the reporter with the WT 3′-UTR of ANGPTL3, but not in the MUT version in HK-2 cells, as seen in Fig. 3B. Consistent with *in vivo* data, a significant increase in miR-144-3p expression was noted in TGF-β1-treated HK-2 cells, as shown in Fig. 3C. Upon miR-144-3p inhibition (Fig. 3D), an increase in ANGPTL3 protein expression was observed in the TGF-β1-stimulated HK-2 cells, as indicated in Fig. 3E.

3.4. Knockdown of ANGPTL3 reversed the effects of miR-144-3p inhibitor on TGF-β1-induced HK-2 cells

To determine if ANGPTL3 is a downstream mediator in the miR-144-3p regulation of TGF-β1-induced RIF *in vitro*, HK-2 cells were transfected with a miR-144-3p inhibitor, either alone or alongside si-ANGPTL3. Initially, we confirmed the reduction of ANGPTL3 in TGF-β1-stimulated HK-2 cells through Western blot analysis, as shown in Fig. 4A. ELISA results revealed that the miR-144-3p inhibitor's reduction of pro-inflammatory factors (TNF-α and IL-6) was significantly reversed by co-transfection with miR-144-3p inhibitor and si-ANGPTL3 in these cells, as indicated in Fig. 4B. Additionally, our data showed that while miR-144-3p knockdown significantly reduced TGF-β1-induced apoptosis in HK-2 cells, this effect was reversed with co-transfection of miR-144-3p inhibitor and si-ANGPTL3, as demonstrated in Fig. 4C. Moreover, the impact of miR-144-3p knockdown on α-SMA, p-PI3K, p-AKT, Collagen I, and Fibronectin in TGF-β1-stimulated HK-2 cells was also negated by si-ANGPTL3 transfection, as depicted in Fig. 4D.

3.5. LY294002 rescued the effects of ANGPTL3 knockdown on TGF-β1-induced HK-2 cells

In exploring how ANGPTL3 influences TGF-β1-induced inflammation and fibrosis in HK-2 cells, we focused on its impact on the PI3K/AKT signaling pathway. We transfected HK-2 cells, stimulated by TGF-β1, with si-ANGPTL3 and then treated them with the

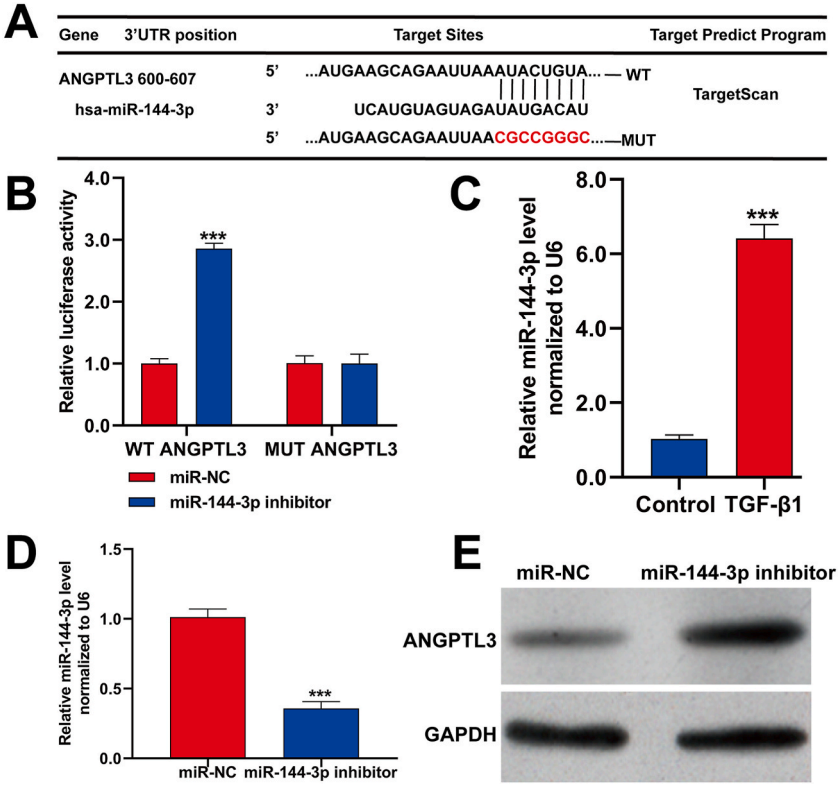

Fig. 3. ANGPTL3 identified as a direct target of miR-144-3p. (A) Binding of miR-144-3p with ANGPTL3 3′-UTR was predicted by TargetScan. (B) Dual luciferase reporter gene assay revealed that miR-144-3p inhibitor significantly increased the luciferase activity of ANGPTL3 wild-type (WT) 3′-UTR. (C) The expression level of miR-144-3p was determined in TGF-β1-stimulated HK-2 cells. The expression level of miR-144-3p (D) and the protein level of ANGPTL3 (E) were measured in HK-2 cells transfected with miR-144-3p inhibitor, followed by TGF-β1 treatment. Data were expressed as means ± SD. ***$p < 0.001$, compared with miR-NC or control.

PI3K/AKT pathway inhibitor LY294002. The results showed that LY294002 significantly reduced the inflammation (Fig. 5A) and apoptosis (Fig. 5B) induced by si-ANGPTL3 in the TGF-β1-stimulated HK-2 cells. On a molecular level, it was observed that the knockdown of ANGPTL3 in these cells led to increased expression of α-SMA, p-PI3K, p-AKT, Collagen I, and Fibronectin, which was subsequently decreased following LY294002 treatment (Fig. 5C). These findings suggest that ANGPTL3 mitigates TGF-β1-induced inflammation and fibrosis in HK-2 cells by inhibiting the PI3K/AKT signaling pathway.

4. Discussion

The involvement of ANGPTL3 in kidney diseases like minimal change nephrotic syndrome and uremic dyslipidemia has been well-documented [11,13]. However, its role in RIF has not been extensively explored. Our study demonstrated a reduction in ANGPTL3 expression in unilateral UUO mice, suggesting its potential link with RIF, corroborating findings from previous research [10]. Obstruction in the ureter frequently causes renal damage and can advance to an irreversible state of RIF, distinguished by the buildup of the extracellular matrix, infiltration of inflammatory cells, and injury and apoptosis of tubular cells [21]. Our laboratory studies showed that increased ANGPTL3 expression in HK-2 cells diminished the inflammation, apoptosis, and fibrosis typically induced by TGF-β1. TGF-β1, identified as a crucial fibrogenic cytokine [22], triggers a cascade of cellular processes that culminate in renal fibrosis. This includes inflammation, oxidative stress, apoptosis, and cell aging, eventually leading to the destruction of proximal tubule cells [23]. Apoptosis is a central process contributing to fibrosis [24], with research indicating that deletion of pro-apoptotic genes Bax and Bak can prevent renal tubular cell apoptosis, thereby safeguarding the tubular cells [25]. Additionally, the heightened presence of inflammatory cells and elevated concentrations of cytokines such as TNF-α, IL-1β and IL-6 are understood to intensify the progression of renal fibrosis [26]. While inflammation serves as a critical defense response to injury, chronic inflammation significantly accelerates fibrotic disease progression [27]. Based on these insights, we hypothesized that ANGPTL3 overexpression could impede renal fibrosis progression by mitigating TGF-β1-induced apoptosis and reducing TNF-α and IL-6 levels.

The modulation of ANGPTL3 expression by miRNAs is an area that has not been extensively explored. The mammalian PI3K/AKT pathway is crucial in cellular processes such as growth, proliferation, survival, and metabolism [28]. Numerous research works have underscored the role of miRNAs in modulating the activation of the PI3K/AKT pathway in renal fibrosis, especially within the context of tubulointerstitial fibrosis. As an example, it has been observed that reduced levels of miR-29c can lead to the suppression of renal

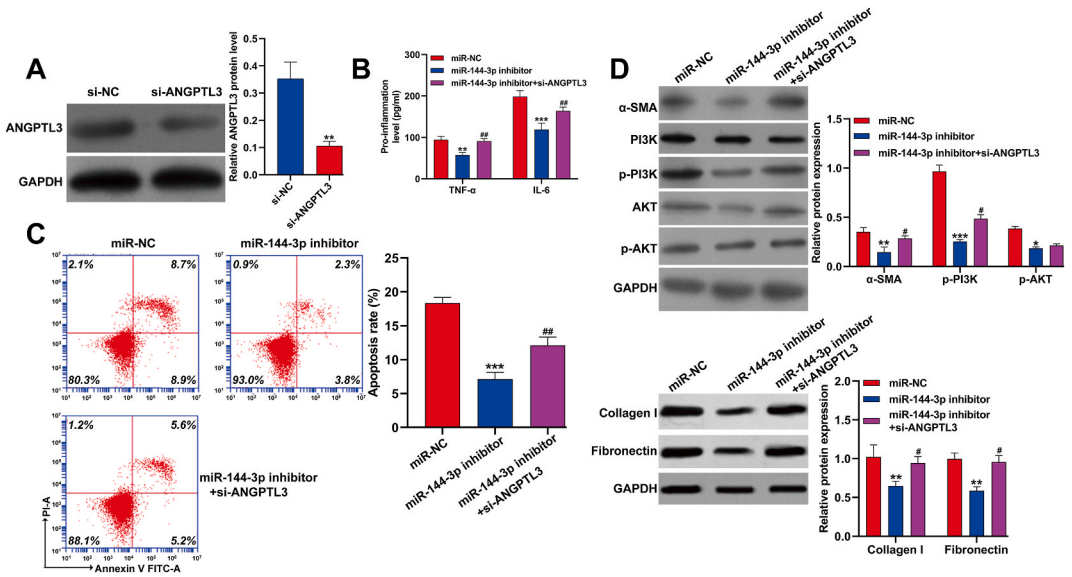

Fig. 4. Knockdown of ANGPTL3 reversed the effects of miR-144-3p inhibitor on TGF-β1-induced HK-2 cells. (A) Knockdown of ANGPTL3 was confirmed via Western blot analysis in TGF-β1-stimulated HK-2 cells transfected with si-ANGPTL3. $^{**}p < 0.01$, compared with si-NC; HK-2 cells were co-transfected with miR-144-3p inhibitor and si-ANGPTL3, followed by treatment with 10 ng/mL TGF-β1. (B) ELISA assay was used to determine the concentration levels of TNF-α and IL-6 in the above HK-2 cells. (C) Cell apoptotic rate was measured in the above HK-2 cells. (D) The protein levels of α-SMA, PI3K, p-PI3K, AKT, p-AKT, Collagen I and Fibronectin were detected in the above HK-2 cells via Western blot analysis. Data were expressed as means ± SD. $^{*}p < 0.05$, $^{**}p < 0.01$, $^{***}p < 0.001$, compared with miR-NC; $\#p < 0.05$, $\#\#p < 0.01$, compared with miR-144-3p inhibitor.

interstitial fibrotic cell proliferation by hindering the PI3K-AKT pathway [29]. Additionally, miR-214-3p knockdown has been found to alleviate renal interstitial fibrosis through the regulation of the PTEN/PI3K/AKT pathway [30]. In diabetic renal fibrosis treatment, miR-466a-3p′s inhibition of the PI3K/AKT pathway plays a role in the therapeutic effects of pentosan polysulfate sodium (PPS) [31]. Our findings are consistent with prior research showing that miR-144-3p contributes to cardiac fibrosis by increasing cell proliferation and collagen synthesis in cardiac fibroblasts through targeting PTEN [17]. Furthermore, the circular RNA circ_0047835 has been associated with the advancement of fibrosis following glaucoma surgery, operating through the miR-144-3p/SP1 axis [32]. Transfecting lung fibroblasts from patients with idiopathic pulmonary fibrosis (IPF) with anti-miR-144-3p led to a rise in RXFP1 expression and a decrease in α-SMA expression [16]. Consequently, our data suggest that miR-144-3p may contribute to TGF-β1-induced renal interstitial fibrosis by targeting ANGPTL3 and influencing the PI3K/AKT signaling pathway. Nonetheless, our study is constrained by several factors: the lack of combined overexpression rescue experiments of miR-144-3p and ANGPTL3 in a laboratory setting, the necessity for Fibronectin staining in live models, and the requirement for more clinical samples to conduct comprehensive *in vivo* experiments. These would provide a clearer understanding of the miR-144-3p/ANGPTL3 interaction in renal interstitial fibrosis.

To sum up, our study suggests that miR-144-3p plays a role in controlling TGF-β1-induced RIF by interacting with ANGPTL3 and influencing the PI3K/AKT signaling pathway. Our findings provide new insights into the mechanisms underlying RIF and identify a promising target for therapy. Developing treatments that specifically target miR-144-3p and ANGPTL3 in the kidneys could markedly alter the treatment strategies for renal fibrosis.

Ethics approval and participation consent

The research received approval from the Animal Ethics Committee at Zhejiang University School of Medicine, adhering to the institution's guidelines for the Use and Care of Experimental Animals (Approval No. ZUS-87DT).

Data availability statement

The data from this study can be obtained from the corresponding author upon a reasonable request.

Funding

This work is supported by Health and Health Science and Technology Program of Zhejiang Province in 2022 (Young Creative Talents Project; NO. 2022RC169).

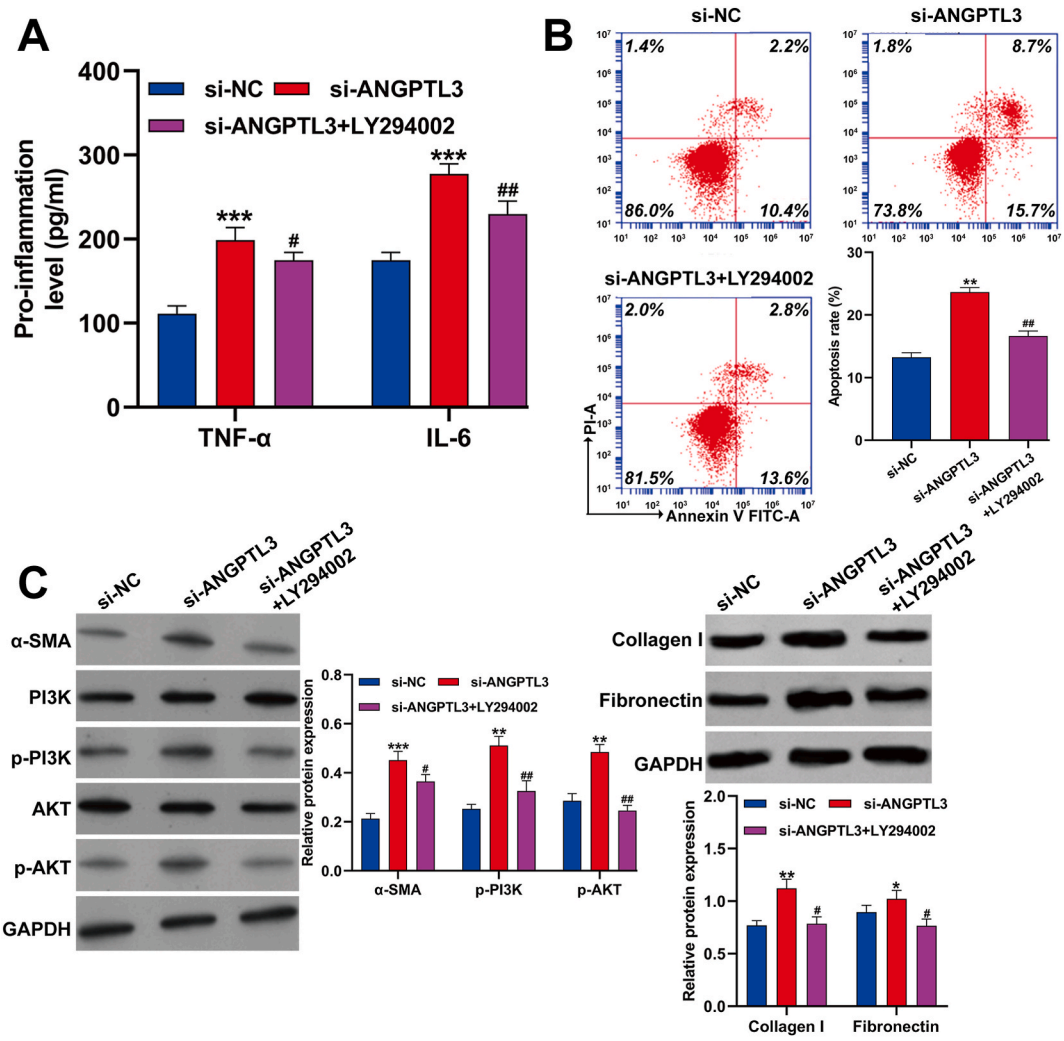

Fig. 5. LY294002 rescued the effects of ANGPTL3 knockdown on TGF-β1-induced HK-2 cells. TGF-β1-stimulated HK-2 cells were transfected with si-ANGPTL3, followed by treatment with PI3K/AKT signaling pathway inhibitor LY294002. (A) ELISA assay was used to determine the concentration levels of TNF-α and IL-6 in the above HK-2 cells. (B) Cell apoptotic rate was measured in the above HK-2 cells. (C) The protein levels of α-SMA, PI3K, p-PI3K, AKT, p-AKT, Collagen I and Fibronectin were detected in the above HK-2 cells via Western blot analysis. Data were expressed as means ± SD. $*p < 0.05$, $**p < 0.01$, $***p < 0.001$, compared with si-NC; $\#p < 0.05$, $\#\#p < 0.01$, compared with si-ANGPTL3.

Patient consent for publication

Not applicable.

CRediT authorship contribution statement

Bin Yang: Writing - original draft, Investigation, Data curation. **Fengxian Shen:** Software, Data curation. **Yi Zhu:** Writing - original draft, Software, Methodology, Formal analysis. **Haolei Cai:** Writing - review & editing, Supervision, Resources, Funding acquisition, Conceptualization.

Declaration of competing interest

The authors declare that they have no known competing financial interests or personal relationships that could have appeared to influence the work reported in this paper.

Acknowledgements

Not applicable.

Appendix ASupplementary data

Supplementary data to this article can be found online at https://doi.org/10.1016/j.heliyon.2024.e24204.

References

[1] A. Nogueira, M.J. Pires, P.A. Oliveira, Pathophysiological mechanisms of renal fibrosis: a review of animal models and therapeutic strategies, In Vivo 31 (2017) 1–22.
[2] S. Yamakoshi, T. Nakamura, N. Mori, C. Suda, M. Kohzuki, O. Ito, Effects of exercise training on renal interstitial fibrosis and renin-angiotensin system in rats with chronic renal failure, J. Hypertens. 39 (2021) 143–152.
[3] H.H. Shi, L.Y. Zhang, L.P. Chen, J.Y. Yang, C.C. Wang, C.H. Xue, Y.M. Wang, T.T. Zhang, EPA-enriched phospholipids alleviate renal interstitial fibrosis in spontaneously hypertensive rats by regulating TGF-beta signaling pathways, Mar. Drugs 20 (2022).
[4] Y.N. Wang, S.X. Ma, Y.Y. Chen, L. Chen, B.L. Liu, Q.Q. Liu, Y.Y. Zhao, Chronic kidney disease: biomarker diagnosis to therapeutic targets, Clin. Chim. Acta 499 (2019) 54–63.
[5] S. Mandard, F. Zandbergen, E. van Straten, W. Wahli, F. Kuipers, M. Müller, S. Kersten, The fasting-induced adipose factor/angiopoietin-like protein 4 is physically associated with lipoproteins and governs plasma lipid levels and adiposity, J. Biol. Chem. 281 (2006) 934–944.
[6] S.M. Azadi, R. Fadaei, R. Omid-Shafaat, J. Hosseini, N. Moradi, Elevated angiopoietin-like protein 3 serum levels in diabetic nephropathy patients and its association with renal function and lipid profile, BMC Nephrol. 24 (2023) 172.
[7] T. Zhao, X. Liang, J. Chen, Y. Bao, A. Wang, X. Gan, X. Lu, L. Wang, ANGPTL3 inhibits renal cell carcinoma metastasis by inhibiting VASP phosphorylation, Biochem. Biophys. Res. Commun. 516 (2019) 880–887.
[8] Y. Ma, J. Liu, H. Liu, X. Han, L. Sun, H. Xu, Podocyte protection by Angptl3 knockout via inhibiting ROS/GRP78 pathway in LPS-induced acute kidney injury, Int. Immunopharm. 105 (2022) 108549.
[9] B. Yang, D. Shi, Y. Chen, Y. Zhu, The potential diagnostic value of immune-related genes in interstitial fibrosis and tubular atrophy after kidney transplantation, Journal of immunology research 2022 (2022) 7212852.
[10] D.G. Maluf, V.R. Mas, K.J. Archer, K. Yanek, E.M. Gibney, A.L. King, A. Cotterell, R.A. Fisher, M.P. Posner, Molecular pathways involved in loss of kidney graft function with tubular atrophy and interstitial fibrosis, Mol. Med. 14 (2008) 276–285.
[11] Y. Li, L. Sun, H. Xu, Z. Fang, W. Yao, W. Guo, J. Rao, X. Zha, Angiopoietin-like protein 3 modulates barrier properties of human glomerular endothelial cells through a possible signaling pathway involving phosphatidylinositol-3 kinase/protein kinase B and integrin alphaVbeta3, Acta Biochim. Biophys. Sin. 40 (2008) 459–465.
[12] D. Mahmood, E. Makoveichuk, S. Nilsson, G. Olivecrona, B. Stegmayr, Response of angiopoietin-like proteins 3 and 4 to hemodialysis, Int. J. Artif. Organs 37 (2014) 13–20.
[13] T. Shoji, S. Hatsuda, S. Tsuchikura, E. Kimoto, R. Kakiya, H. Tahara, H. Koyama, M. Emoto, T. Tabata, Y. Nishizawa, Plasma angiopoietin-like protein 3 (ANGPTL3) concentration is associated with uremic dyslipidemia, Atherosclerosis 207 (2009) 579–584.
[14] X. Li, Z.Q. Dong, H. Chang, H.B. Zhou, J. Wang, Z.J. Yang, M. Qiu, W.F. Bai, S.L. Shi, Screening and identification of key microRNAs and regulatory pathways associated with the renal fibrosis process, Molecular omics 18 (2022) 520–533.
[15] W. Lv, F. Fan, Y. Wang, E. Gonzalez-Fernandez, C. Wang, L. Yang, G.W. Booz, R.J. Roman, Therapeutic potential of microRNAs for the treatment of renal fibrosis and CKD, Physiol. Genom. 50 (2018) 20–34.
[16] H. Bahudhanapati, J. Tan, J.A. Dutta, S.B. Strock, J. Sembrat, D. Alvarez, M. Rojas, B. Jager, A. Prasse, Y. Zhang, et al., MicroRNA-144-3p targets relaxin/insulin-like family peptide receptor 1 (RXFP1) expression in lung fibroblasts from patients with idiopathic pulmonary fibrosis, J. Biol. Chem. 294 (2019) 5008–5022.
[17] X. Yuan, J. Pan, L. Wen, B. Gong, J. Li, H. Gao, W. Tan, S. Liang, H. Zhang, X. Wang, MiR-144-3p enhances cardiac fibrosis after myocardial infarction by targeting PTEN, Front. Cell Dev. Biol. 7 (2019) 249.
[18] E. Martínez-Klimova, O.E. Aparicio-Trejo, E. Tapia, J. Pedraza-Chaverri, Unilateral ureteral obstruction as a model to investigate fibrosis-attenuating treatments, Biomolecules 9 (2019).
[19] K. Yanai, S. Kaneko, H. Ishii, A. Aomatsu, K. Ito, K. Hirai, S. Ookawara, K. Ishibashi, Y. Morishita, Quantitative real-time PCR evaluation of microRNA expressions in mouse kidney with unilateral ureteral obstruction, J. Vis. Exp. (2020).
[20] K.J. Livak, T.D. Schmittgen, Analysis of relative gene expression data using real-time quantitative PCR and the 2(-Delta Delta C(T)) Method, Methods 25 (2001) 402–408.
[21] H. Matsuda, T. Mori, D. Kurumazuka, K. Kitada, T. Hayashi, K. Nagatoya, T. Inoue, A. Ukimura, Y. Matsumura, N. Ishizaka, et al., Inhibitory effects of T/L-type calcium channel blockers on tubulointerstitial fibrosis in obstructed kidneys in rats, Urology 77 (2011), 249 e249-215.
[22] M. Sato, Y. Muragaki, S. Saika, A.B. Roberts, A. Ooshima, Targeted disruption of TGF-beta 1/Smad 3 signaling protects against renal tubulointerstitial fibrosis induced by unilateral ureteral obstruction, J. Clin. Invest. 112 (2003) 1486–1494.
[23] D. Portilla, Apoptosis, fibrosis and senescence, Nephron Clin. Pract. 127 (2014) 65–69.
[24] A. Johnson, L.A. DiPietro, Apoptosis and angiogenesis: an evolving mechanism for fibrosis, Faseb. J. 27 (2013) 3893–3901.
[25] Q. Wei, G. Dong, J.K. Chen, G. Ramesh, Z. Dong, Bax and Bak have critical roles in ischemic acute kidney injury in global and proximal tubule-specific knockout mouse models, Kidney Int. 84 (2013) 138–148.
[26] R. Li, Y. Guo, Y. Zhang, X. Zhang, L. Zhu, T. Yan, Salidroside ameliorates renal interstitial fibrosis by inhibiting the TLR4/NF-kappaB and MAPK signaling pathways, Int. J. Mol. Sci. 20 (2019).
[27] C. Nathan, A. Ding, Nonresolving inflammation, Cell 140 (2010) 871–882.
[28] B. Hassan, A. Akcakanat, A.M. Holder, F. Meric-Bernstam, Targeting the PI3-kinase/Akt/mTOR signaling pathway, Surg. Oncol. Clin. 22 (2013) 641–664.
[29] W. Feng, H. Xie, J. Li, X. Yan, S. Zhu, S. Sun, miR-29c inhibits renal interstitial fibrotic proliferative properties through PI3K-AKT pathway, Appl. Bionics Biomechanics 2022 (2022) 6382323.
[30] D. Hou, Q. Wu, S. Wang, S. Pang, H. Liang, H. Lyu, L. Zhou, Q. Wang, L. Hao, Knockdown of miR-214 alleviates renal interstitial fibrosis by targeting the regulation of the PTEN/PI3K/AKT signalling pathway, Oxid. Med. Cell. Longev. 2022 (2022) 7553928.
[31] L. Xiao, A. Chen, Q. Gao, B. Xu, X. Guo, T. Guan, Pentosan polysulfate ameliorates fibrosis and inflammation markers in SV40 MES13 cells by suppressing activation of PI3K/AKT pathway via miR-446a-3p, BMC Nephrol. 23 (2022) 105.
[32] H. Cao, X. Xu, K. Wang, C. Li, Circ_0047835 combines with miR-144-3p to promote the proliferation, invasion, migration, and fibrosis of TGF-beta 1-treated human tenon's capsule fibroblasts by upregulating SP1, Curr. Eye Res. (2023) 1–11.